Pergamon

Int. J. Heat Mass Transfer. Vol. 40, No. 9, pp. 2201–2217, 1997

0017–9310/97 $17.00+0.00

PII: S0017–9310(96)00190–1

The effect of coarse particles on the heat transfer in a turbulent boundary layer

G. HETSRONI, R. ROZENBLIT and L. P. YARIN

Department of Mechanical Engineering, Technion—Israel Institute of Technology, Haifa 32000, Israel

(*Received* 14 *September* 1995 *and in final form* 13 *May* 1996)

Abstract—This paper deals with the effect of coarse particles on heat transfer in a turbulent boundary layer. The temperature of the wall, in the presence of coarse particles in the near-wall flow, is studied by using infrared thermography. Experimental data on the heat transfer coefficient are obtained. A possible mechanism of heat transfer in the presence of coarse particles in the near-wall region of a turbulent boundary layer is discussed. © 1997 Elsevier Science Ltd. All rights reserved.

1. INTRODUCTION

The interaction of a near-wall flow with submerged bodies such as coarse particles, elements of roughness, etc. is of great importance for understanding momentum and heat transfer in particle-laden flows and turbulent boundary layers developing over rough surfaces. Such an interaction is accompanied by changes in the flow field and modification of its hydrodynamic and thermal characteristics, including heat transfer.

It is well known that the near-wall region possesses a rather complicated structure [1–3], which results from a strong interaction of large-scale vortices, in the core of the turbulent boundary layer, with low-speed streaks which exist in its sublayer [4–6]. Such an interaction leads to drastic changes of the flow field: the low-speed streaks migrate away from the wall, oscillate and break-up, resulting in burst formation. This process is accompanied by penetration of high-velocity fluid into the near-wall region and ejection of low-velocity fluid from the wall [4, 7–9].

As a result of the bursting process, an intensive motion of fluid normal to the wall occurs. This motion is the major contribution to the turbulence production process in the turbulent core. It is also responsible for the energy transport from the time-averaged velocity to the fluctuational one and heat transfer from the wall [10].

At present, there are a number of publications dealing with coarse particle–turbulence interaction [11–12]. Measurements [13–18] showed that turbulent intensity in particle-laden flows with coarse particles is larger than that in particle-free flows. Hetsroni [12] suggested that this effect could be explained by a vortex shedding phenomenon. The latter results from turbulent wake formation behind coarse particles. This idea was used later by Yarin and Hetsroni [19] to describe turbulent modulation in various types of particle-laden flows.

The experiments of Rashidi *et al.* [20] and Kaftori [21] showed that particle–turbulence interaction manifests itself not only in a change of turbulent fluctuations but also in a change of coherent structures of the flow and bursting. An effect of wall roughness on vortical structures and coherent motion in a turbulent flow has been studied by Grass *et al.* [22].

An effect of coarse particles on the thermal structure of a near-wall region of the turbulent boundary layer has been investigated by Hetsroni and Rozenblit [23]. Their experiments showed that coarse particles, present close to the wall, lead to a rearrangement of the temperature field on the wall. The latter manifests itself in a change of temperature fluctuations on the wall, and spanwise temperature streak-spacing, as well as in variation of the heat transfer coefficient.

Detailed data on the effect of coarse particles, located on the wall, on the heat transfer in a turbulent boundary-layer, have been obtained by Hetsroni *et al.* [24]. It was shown that near a coarse particle the heat transfer coefficient increases 1.5–3 times. It was hypothesized that the increase in the heat transfer rate was due to the relative velocity between the particles and the fluid near the wall, which caused an inrush of cold fluid into the wall region. This effect can be maximized by making the particles stationary.

The effect of roughness on the heat transfer in a turbulent boundary layer was a subject of a number of other publications, e.g. Owen and Thomson [25], Yaglom and Kader [26], Hirota *et al.* [27], Zukauskas [28], etc. Numerous works are devoted to the effect of coarse roughness, of various types and geometries, on the flow field e.g. ref. [29]. The results show that coarse roughness has a strong effect on the flow characteristics. A number of theoretical and experimental investigations on the effect of coarse roughness of

NOMENCLATURE

c_p	specific heat of the fluid at constant pressure
d	the particle diameter
D	the distance between strings of coarse particles
h	the distance between a particle center and the wall
$\bar{h}, h^+$	non-dimensional distance from the particle center to the wall, $\bar{h} = h/d$, $h^+ = hu^*/\nu$
H	the depth of the fluid layer
ℓ	distance between particles in a string
Nu_ξ	the Nusselt number, $Nu_\xi = \alpha_0 d/\lambda$
Nu_0	the Nusselt number at the location of particle center
$\bar{Nu}_\xi$	dimensionless value of the Nusselt number, $\bar{Nu}_\xi = Nu_\xi/Nu_0$
Pr	the Prandtl number, $Pr = \mu c_p/\lambda$
Re_H	the Reynolds number $Re_H = UH/\nu$
Re^*	the Reynolds number, $Re^* = u^* d/\nu$
r	radial coordinate in a cylindrical coordinate system
t	temperature
u^*	shear velocity
u_∞	free stream velocity
U	mean flow velocity
v_r, v_φ	radial and azimuthal components of the velocity vector
v	velocity vector
v_r', v_φ'	radial and azimuthal components of the velocity fluctuations
x,y	longitudinal and vertical Cartesian coordinates
x_o	distance from the leading edge of plate to the center of the particle
y^+	non-dimensional distance from the wall, $y^+ = yu^*/\nu$.

Greek symbols

α	local heat transfer coefficient
α_∞	heat transfer coefficient in undisturbed flow
α_0	excess heat transfer coefficient, $\alpha_0 = \alpha - \alpha_\infty$
α_m	maximum heat transfer coefficient
$\bar{\alpha}_m$	dimensionless maximum heat transfer coefficient, $\bar{\alpha}_m = \alpha_m/\alpha_\infty$
α_{0m}	maximum of the excess heat transfer coefficient, $\alpha_{0m} = \alpha_m - \alpha_\infty$
$\bar{\alpha}$	dimensionless heat transfer coefficient $\bar{\alpha} = \alpha/\alpha_\infty$
$\bar{\alpha}_{0m}$	dimensionless excess heat transfer coefficient, $\bar{\alpha}_{0m} = \alpha_0/\alpha_{0m}$
δ	boundary layer thickness
ε	level of temperature fluctuations on the wall (RMS)
ε_∞	level of temperature fluctuations on the wall in undisturbed flow
ε_0	level of excess temperature fluctuations on the wall, $\varepsilon_0 = \varepsilon - \varepsilon_\infty$
ε_m	level of maximum temperatures fluctuation on the wall
ε_{min}	level of minimum temperature fluctuations on the wall
ε_{0m}	level of maximum excess temperature fluctuations on the wall, $\varepsilon_{0m} = \varepsilon_m - \varepsilon_\infty$
$\bar{\varepsilon}$	level of dimensionless temperature fluctuation on the wall, $\bar{\varepsilon} = \varepsilon/\varepsilon_\infty$
$\bar{\varepsilon}_m$	level of maximum dimensionless temperature fluctuations on the wall, $\bar{\varepsilon}_m = \varepsilon_m/\varepsilon_\infty$
$\bar{\varepsilon}_{min}$	level of minimum dimensionless temperature fluctuations on the wall, $\bar{\varepsilon}_{min} = \varepsilon_{min}/\varepsilon_\infty$
$\bar{\varepsilon}_{0m}$	level of dimenionless excess temperature fluctuations on the wall, $\bar{\varepsilon}_{0m} = \varepsilon_0/\varepsilon_{0m}$
λ	the thermal conductivity of the fluid
μ	dynamic viscosity
ν	kinematic viscosity
ξ	longitudinal coordinate from the particle
$\bar{\xi}$	non-dimensional longitudinal coordinate normalized to the particle diameter, $\bar{\xi} = \xi/d$
$\tilde{\xi}$	non-dimensional longitudinal coordinate normalized to the distance from the particle center to the wall, $\tilde{\xi} = \xi/h$
$\tilde{\xi}_m$	non-dimensional longitudinal coordinate corresponding to the maximum of $\bar{\alpha}$
Π	non-dimensional group
ρ	fluid density
φ	angular coordinate in a cylindrical coordinate system.

various types (particles, ribs, etc.) on heat transfer are available [30–32]. Also, a number of effective heat exchangers in which the heat transfer is enhanced by using coarse roughness were reviewed by Webb [33].

The aim of the present study is to evaluate the effect of coarse particles on the heat transfer rate in a turbulent boundary layer. First, we determine the heat transfer coefficient in a turbulent boundary layer in the presence of a single stationary particle. Then we study the interaction of a number of coarse particles

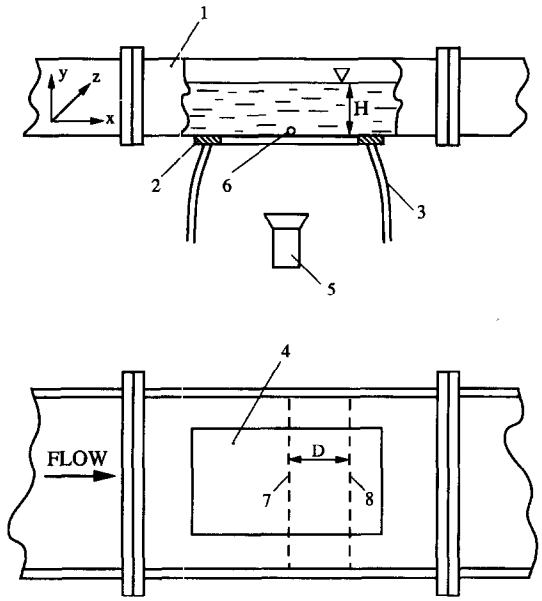

Fig. 1. Test section for the I.R. visualization. 1 flume; 2 frame; 3 power cables; 4 constantan foil; 5 I.R. scanner; 6 research object (single coarse particle, array of coarse particles, cylinder); 7 location of the first array of the coarse particles; 8 location of the second array of the coarse particles (in experiments with two arrays).

(arranged in an array) and their effect on heat transfer. We also consider a possible mechanism for enhancement of heat transfer in the presence of coarse particles.

2. EXPERIMENTAL SET-UP

The experimental set-up and measurement technique were described in detail elsewhere [23]. Therefore, we present here only the main parameters see Fig. 1. The flow loop is a stainless steel open flume 4.3 m long, 0.32 m wide and 0.1 m deep. Water of constant temperature is recirculated in it, with the flow rate being measured by means of a flowmeter. The heater is located at the bottom of the test section. It is a strained constantan foil on an insulated frame (0.33 m long, 0.2 m wide and 50 μm thick). The internal dimensions of the frame are 0.3×0.15 m (Fig. 1). The foil is attached to the window by means of contact adhesive and is coated on the air side with black matt paint of about 20 μm thickness. Heat flux ($q = 1.01$ W cm^{-2}) was achieved by supplying d.c. power to the foil of up to 300 A.

The actual temperature distribution on the heater surface is measured by an I.R. imaging radiometer. The temperature range of the radiometer is from -20 to 1500°C, with a minimum detectable temperature difference of 0.1°C at 30°C. Through calibration, the thermal imaging was made very accurate in a narrow temperature range, giving a typical noise equivalent to temperature difference (NETD) of less than 0.2°C (with image average less than 0.05°C). A typical horizontal resolution was 1.8 mrad or 256 pixels/line.

Fully developed flow was established in the region beyond 2.5 m downstream from the entrance of the flume, which was confirmed by measurements of the velocity distribution. The flow parameters: mean velocity U [m s^{-1}], mean temperature t [°C], flow depth H [m], and shear velocity u^* [m s^{-1}], varied within the limits $0.078 \leqslant U \leqslant 0.226$, $20 \leqslant t \leqslant 23$, $0.037 \leqslant H \leqslant 0.07$ and $0.0042 \leqslant u^* \leqslant 0.0121$. The measurements show that the temperature gradient along the foil did not exceed 6 K m^{-1}. Accordingly, the conductive to convective heat flux ratio has an order of 10^{-6}. Thus, the effect of conductivity of the foil material is negligible.

A hot film anemometer with a standard single-sensor boundary-probe was used for the mean profile measurement. The probe was connected to a traversing mechanism having a spatial resolution of 10 μm. The signal of the anemometer was transmitted in digital code through an acquisitor to a PC. The streamwise velocity profiles were then employed to determine values of the shear velocity u^*, by means of Clauser-type fits.

The scanner of the I.R. radiometer was located *under* the heater foil at a distance of about 0.5 m. It was shown [23] that the thermal field on the air side of the heated foil is almost the same as the temperature pattern on the bottom of the flume. A distortion in the measured values of the temperature fluctuations begins at frequencies higher than 15–20 Hz, whereas the characteristic frequency of the observed phenomena are of the order of 1 Hz.

Two series of experiments were carried out. In the first, heat removal from the wall, in the presence of a single particle on its surface, was investigated. In the second, we studied the effect on heat transfer of a number of particles located on the foil surface, or at various distances from it.

A single particle, as well as a string of particles, were located (motionless) on the heated surface at a distance of 0.18 m from the leading edge of the heater. Steel, glass and polyethylene particles were used. The particle diameter d [mm], thermal conductivity λ [W m^{-1} K^{-1}], specific heat c_p [J g^{-1} K^{-1}] and density γ [g cm^{-3}] varied within the limits: $1.2 \leqslant d \leqslant 5.0$, $0.42 \leqslant \lambda \leqslant 39.2$, $0.49 \leqslant c_p \leqslant 0.67$ and $1.25 \leqslant \gamma \leqslant 7.9$. The heavy particles (steel, glass) were motionless on the heated surface, due to gravity. The maximum flow velocity was chosen so that the particles were motionless.

The temperature distribution upstream and downstream of the particle was measured along its center line. For the quantitative analysis the 'point mode' of the I.R. radiometer was used. The temperature at a point was transmitted, in a digital code, to a PC. During each run, a sequence of at least 200 s was recorded. The sampling period of the temperature data was 0.05 s. Both the time average temperature at the point and the r.m.s. temperature fluctuations

within each run were studied. Simultaneously, the thermal pattern was recorded on a video. The video was then used in playback mode to analyze the data, i.e. to determine the influence of the particle on the time-averaged temperature field and the turbulence structure near the wall.

In the second series of experiments, a horizontal wire was used, on which plastic particles of diameter $d = 5.0$ mm were strung with a pitch of $\Delta z = 8.0$ mm. The string was located, in the spanwise direction, at a distance of 0.22 m from the leading edge of the heater and could be moved up and down between the bottom of the flume and its interface. The uncertainty in the vertical location of the string was $\delta y^+ \leqslant 1.5$ (δy^+ is the uncertainty of y^+, $y^+ = yu^*/v$ is the dimensionless distance from the wall, y is the distance from the wall, u^* is the shear velocity and v is the kinematic viscosity). The diameter of the wire supporting the spheres was $d_w = 0.3$ mm. The Reynolds number was $Re_w = u^* d_w/v \leqslant 2.5$. At such Re_w, micro-scale disturbances generated by the wire damped very quickly and have practically no effect on the flow field. At low flow velocity no vibration of the string was observed.

In the presence of a number of particles on the foil surface, the data on the average (over the surface) heat transfer coefficient are important. Therefore, in this case the 'area mode' of the I.R. radiometer was used. The elementary area was a strip 0.15 m long (in the spanwise direction of the flume) and 6 mm wide. The strip was moved along the flow direction (upstream and downstream of the particles). The time–area average temperature at each strip position was studied and the thermal pattern was recorded on a video.

3. DIMENSIONAL ANALYSIS

Heat transfer in a turbulent boundary layer depends on the flow structure and the physical properties of the fluid. When a single coarse particle (or cluster of particles) is located on the wall surface, the rate of heat transfer also depends on the particle shape and location. There is no effect of the particle material on the heat transfer.

The coarse particles affect heat transfer via their influence on the near-wall flow, which plays an important role in the transport processes occurring in the turbulent boundary layer. As was mentioned above, the near wall flow possesses a rather complicated structure, which results from the interaction of large-scale vortices with low-speed streaks in the sublayer.

The mechanism by which the particles affect the heat transfer is outlined as follows. The particles located in the turbulent boundary layer generate strong disturbances which affect the near-wall flow, i.e. they cause inrush of a cold fluid from the mainstream into the boundary layer. This flow affects the streamwise as well as the spanwise velocities, which, in turn, may affect the bursting frequency and thus, have a profound effect on the heat transfer from the wall [24].

In this section a qualitative analysis of the effect of particles on the heat transfer in a turbulent boundary layer is performed. We determine the functional dependence of the heat transfer coefficient, near a coarse particle, on the flow parameters. Discussion on the mechanism of the effect of a coarse particle on the heat transfer in a turbulent boundary layer is given below in Section 5.

First consider the case in which a single coarse particle is located on the wall (Fig. 2(a)). Suppose that the coarse particle is a sphere of diameter d. Also, assume that the size of the particle exceeds the thickness of the viscous sublayer. However, it is smaller than the thickness of the turbulent boundary layer, which means that the particle diameter changes with the range $10 \leqslant d^+ \leqslant 500$, where $d^+ = du^*/v = Re^*$.

As a velocity scale in the near-wall region, we use the shear velocity u^* and as a scale of length, we use the particle diameter d. Thus, we have the following set of governing parameters

$$\alpha = \alpha(\alpha_0, u^*, \rho, \mu, \lambda, c_p, d, \xi) \tag{1}$$

where $\alpha_0 = \alpha - \alpha_\infty$ is the excess heat transfer coefficient, α and α_∞ are the heat transfer coefficients near the particle and in the undisturbed flow, respectively: ρ, μ, λ, c_p are the density, viscosity, thermal conductivity and specific heat of the fluid, respectively: $\xi = x - x_0$, x is the longitudinal coordinate, x_0 is the distance from the leading edge of the plate to the center of the particle.

It is seen from equation (1) that the problem at hand is governed by eight parameters, four of which possess independent dimensions. Using the Buckingham π-theorem the number of non-dimensional parameters in this problem can be reduced to the following four groups

$$\Pi_1 = \xi/d, \Pi_2 = \alpha_0/u^* \rho c_p, \Pi_3 = u^* d\rho/\mu, \Pi_4 = \alpha_0 d/\lambda. \tag{2}$$

Since $u^* d/v = Re^*$, $\alpha_0 d/\lambda = Nu_\xi$, $\mu c_p/\lambda = Pr$, we can write the following functional dependence between the non-dimensional groups of equation (2) in the form

$$Nu_\xi = F_1(\bar{\xi}, Re^*, Pr) \tag{3}$$

where Nu_ξ is the 'effective' Nusselt number characterizing the excess heat transfer rate under the effect of a coarse particle, compared to that in the undisturbed flow and $\bar{\xi} = \xi/d$. Thus, the local Nusselt number is a function of the particle Reynolds number, the properties of the fluid and the location.

Experimental data on the heat transfer in a turbulent boundary layer near the location of a coarse particle (see Section 4), show that equation (3) may be presented as a product of two functions: one of them depending only on Re^*, and the second on $\bar{\xi}$ and Pr. Accordingly, equation (3) is written in the following form:

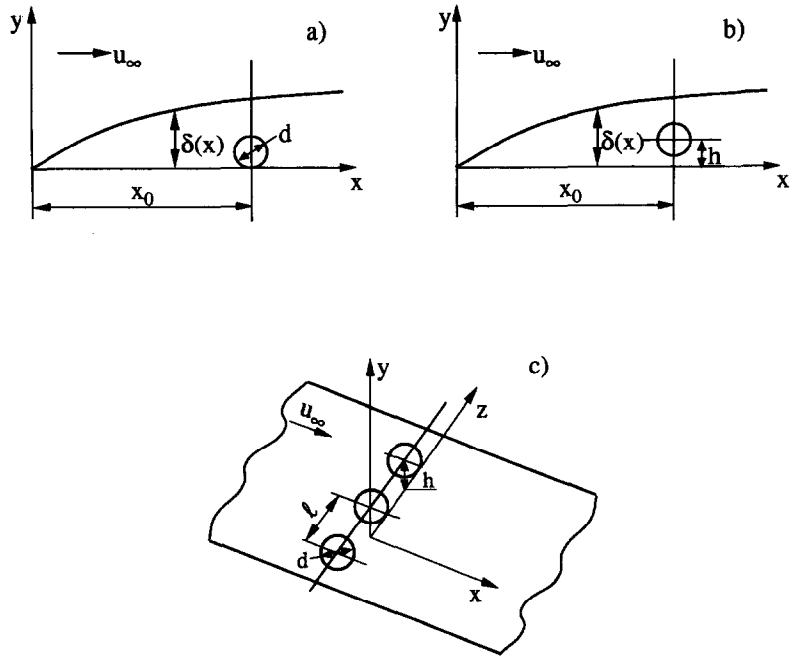

Fig. 2. Coordinate system associated with the coarse particles near the wall. (a) Single coarse particle on the wall; (b) single coarse particle elevated above the wall; (c) array of coarse particles above the wall.

$$Nu_\xi = \varphi_1(Re^*) f_1(\bar{\xi}, Pr). \quad (4)$$

The Nusselt number depends only on the parameters Re^* and Pr as $\bar{\xi} \to 0$; thus, $Nu_\xi \to Nu_m = \varphi_1(Re^*) f_1(Pr)$. Hence, equation (4) can be rearranged as follows:

$$\tilde{N}u_\xi = \Psi_1(\xi, Pr) \quad (5)$$

where $\tilde{N}u_\xi = Nu_\xi/Nu_m$, Ψ_1 is a function which possesses the following features:

$$\Psi_1(\bar{\xi}, Pr) \to 1 \text{ at } \bar{\xi} \to 0: \quad \Psi_1(\bar{\xi}, Pr) \to 0 \text{ at } \bar{\xi} \gg 1 \quad (6)$$

and is independent of the particle size and the location, relative to the leading edge of the plate.

As is seen from equation (5), a distribution of the heat transfer coefficient close to a coarse particle depends on $\bar{\xi}$ only (when physical properties of the fluid are fixed).

When a single coarse particle, or a string of coarse particles, is located above the wall (Figs 2(b)–(c)), we obtain the following functional dependences:

$$\tilde{N}u_\xi = \Psi_2(\bar{\xi}, Pr) \quad (7)$$

$$\tilde{N}u_\xi = \Psi_3(\bar{\xi}, Pr, \bar{\ell}) \quad (8)$$

where $\bar{\xi} = \bar{\xi}/\bar{h}$, $\bar{h} = h/d$, h is the distance from the center of the particle to the wall, $\bar{\ell} = \ell/d$, ℓ is the distance between neighbouring particles in the string.

Thus, under given conditions, with Pr and $\bar{\ell}$ fixed, the distribution of the heat transfer coefficient near a single coarse particle or an array of coarse particles above the wall is determined by one variable, $\bar{\xi}$, only.

4. HEAT TRANSFER COEFFICIENT

4.1. *A single coarse particle*

The experimental data on the thermal field of the heated foil, near the location of a single coarse particle, are shown in Fig. 3†, where the regions of higher and lower temperature can be seen. Variation of the heat transfer coefficient $\bar{\alpha}$ (the value of the local heat transfer coefficient α [W m^{-2} K^{-1}] is changed, $650 < \alpha < 2000$) and temperature fluctuations on the wall $\bar{\varepsilon}$ as a function of non-dimensional variable $\bar{\xi}$ are illustrated in Fig. 4(a)‡. It is seen that the effect of a single coarse particle on the heat transfer coefficient is observed only close to the particle. A sharp increase in $\bar{\alpha}$ is observed in front of the particle (within the limits $-1 < \bar{\xi} < -0.25$) where the heat transfer coefficient is three times larger than that in the undisturbed flow. A similar effect is also observed when a macro-scale body (for example, square or circular columns) is present in the turbulent boundary layer [34]. Note also the maximum of the curve $\bar{\alpha}(\bar{\xi})$ is shifted to the left from the particle center. The heat transfer coefficient decreases at $\bar{\xi} > \bar{\xi}_m$ ($\bar{\xi}_m$ is the non-dimensional coordinate corresponding to the maximum of $\bar{\alpha}$). It decreases so rapidly, that in some region of a flow behind the particle, $\bar{\alpha}$ becomes less

† In Figs. 3, 7, 10 the color shades are indicative of the temperatures. The data in Figs. 4–9 correspond to measurement along an axis through the particle center.

‡ In the study of heat transfer in a turbulent boundary layer over a heated wall, we estimated the effect of natural convection. It was shown that this effect is negligible when the velocity is higher than 0.1 m s^{-1}.

than that in the unperturbed flow ($\bar{\alpha} < 1$). This phenomenon was observed under different conditions of heat transfer, particle sizes, flow velocity, etc.

The zone with a significant variation of temperature fluctuations is larger than the zone with a noticeable change of the heat transfer coefficient ($-4 < \bar{\xi} < 8$). In a certain region ($-4 < \bar{\xi} < -1$), in front of the particle, the level of temperature fluctuations exceeds that in the unperturbed flow. Within the limits $-1 < \bar{\xi} < -0.25$, a sharp drop in temperature fluctuations takes place. The minimum in the dependence $\bar{\varepsilon}(\bar{\xi})$ corresponds approximately to $\bar{\xi} = -0.25$. At $\bar{\xi} > -0.25$, an increase of the temperature fluctuations to the value corresponding to the unperturbed flow, is observed.

The experimental data on the heat transfer coefficient corresponding to various particle sizes plotted in Fig. 4(b) in a form predicted by the dimensional analysis. In this figure the data on the distribution of the heat transfer coefficient $\bar{\alpha}_{0m}$, near coarse particles of various sizes, are presented. As can be seen from the figure, the experimental data corresponding to particles of different sizes group around a single curve $\bar{\alpha}_{0m} = f(\bar{\xi})$.

The distribution of temperature fluctuations on the heated foil near a single coarse particle is shown in Fig. 4(b). In spite of the significant scatter of experimental data for different particle sizes, these data allow us to understand some specifics of the effect of coarse particles on temperature fluctuations in the near wall zone. The data show that there are two regions near a single coarse particle in which temperature fluctuations differ from those in the unperturbed flow. In front of the particle, an enhancement of temperature fluctuations is observed. The maximum of temperature fluctuations corresponds to the non-dimensional distance from the center of the particle equal approximately to $\bar{\xi} = -1.5$. Behind the particle, temperature fluctuations are suppressed. The sharp drop in the temperature fluctuations occurs within a narrow domain corresponding to $-0.6 < \bar{\xi} < +0.2$. Comparison of the data for the heat transfer coefficient and temperature fluctuations shows that the extent of enhancement and suppression regions of temperature fluctuations is larger than the corresponding region for the heat transfer coefficient. This fact points out that temperature fluctuations are more sensitive to hydrodynamic disturbances, generated by a coarse particle, than the heat transfer coefficient.

The dependences of $\bar{\alpha}_m$ and $\bar{\varepsilon}_m$, for particles of different sizes vs Re^*, are plotted in Figs. 5(a)–5(b), where the heat transfer coefficient is shown to depend strongly on Re^*. An increase in Re^* leads to an increase in α_m, whereas $\bar{\varepsilon}_m$ (Re^*) and $\bar{\varepsilon}_{min}$ (Re^*) depend weakly on Re^*.

4.2. *String of coarse particles*

The effect of a string of particles, located on the surface of the heated foil or at some elevation above it, on the thermal field of the heated foil and the heat transfer in a turbulent boundary layer, is illustrated in Figs 6–8. Note that there exists a second maximum in $\bar{\alpha}(\bar{\xi})$ and $\bar{\alpha}_{0m}(\bar{\xi})$. The absolute values of these maxima are inversely proportional to the particle elevation h above the foil. An increase in h is also accompanied by a noticeable shift in the second maximum downstream, whereas the location of the first maximum is practically independent of h.

The experimental data on the heat transfer in a turbulent boundary layer in the presence of a string of coarse particles is plotted in Fig. 8, in a form suggested by the dimensional analysis. It is seen that the data corresponding to different elevations of the particle string group near a single curve $\bar{\alpha}_{0m} = f(\bar{\xi})$ in the $\bar{\alpha}_{0m}$, $\bar{\xi}$ plane. This curve depicts the influence of a string of coarse particles on the heat transfer. As can be seen from Fig. 8, the effect of the string of the coarse particles is negligible far in front of the particles (for $\bar{\xi} < -8$). In the range $-8 < \bar{\xi} < -0.5$ a weak decrease in the heat transfer coefficient is observed. Near the string of the particles (within the limits $-0.5 < \bar{\xi} < 0$) a sharp increase followed by a drop ($0 < \bar{\xi} < 1$) in the heat transfer coefficient takes place. In a wide region behind the string of particles (within the limits $2 < \bar{\xi} < 7$) the heat transfer coefficient increases once again. The second maximum of $\bar{\alpha}_{0m} = f(\bar{\xi})$ is located at $\bar{\xi} = 7$. At $\bar{\xi} > 7$ the heat transfer coefficient decreases monotonically to the value corresponding to the unperturbed flow.

The measurements show that an increase of elevation of the string of coarse particles $h^+ = hu^*/\nu$ is accompanied by a decrease in the second maximum, and an almost invariable first maximum. An increase in $\bar{h}$ is also accompanied by a significant shift of the second maximum and practically no change in the location of the first one.

The data show that a change in the Reynolds number as well as in the depth of the fluid layer affects the distribution of the heat transfer coefficient only slightly: the data corresponding to different values of Re_H (or H) group near a single curve.

4.3. *Two strings of coarse particles*

The effect of two strings of coarse particles on the heat transfer in a turbulent boundary layer is illustrated in Figs 9 and 10. In this case the dependences of $\bar{\alpha}_{0m} = f(\bar{\xi})$ also have two maxima corresponding to the first and the second string of particles. There is a noticeable difference in the distributions of the heat transfer coefficient at small and high Reynolds numbers. This difference manifests itself more clearly in the region behind the second maximum. At high Reynolds numbers, disturbance damping by the coarse particles is weaker. An increase in the distance between the strings of particles leads to a widening of the region where the heat transfer coefficient is higher than that in the unperturbed flow.

4.4. *Cylindrical roughness*

The effect of cylindrical roughness (a single cylinder oriented in the spanwise direction) on the heat transfer

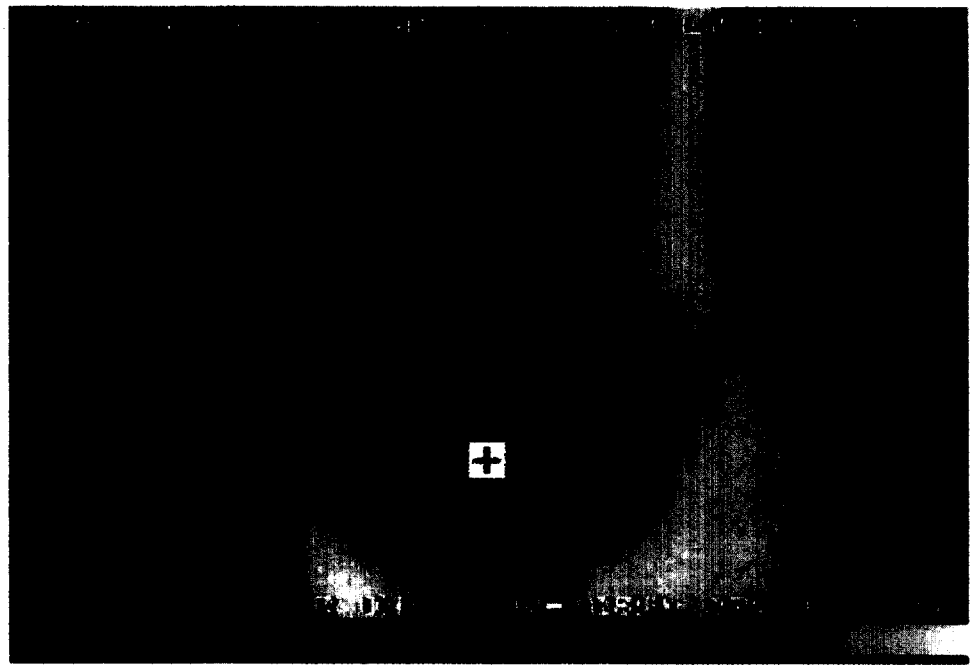

Fig. 3. The thermal field of the heated foil near the location of the single coarse particle. $Re_H = 5150$, $d = 4.75$ mm. The flow direction is from the bottom to the top. The color play interval is 10°C. The particle is located at '+'.

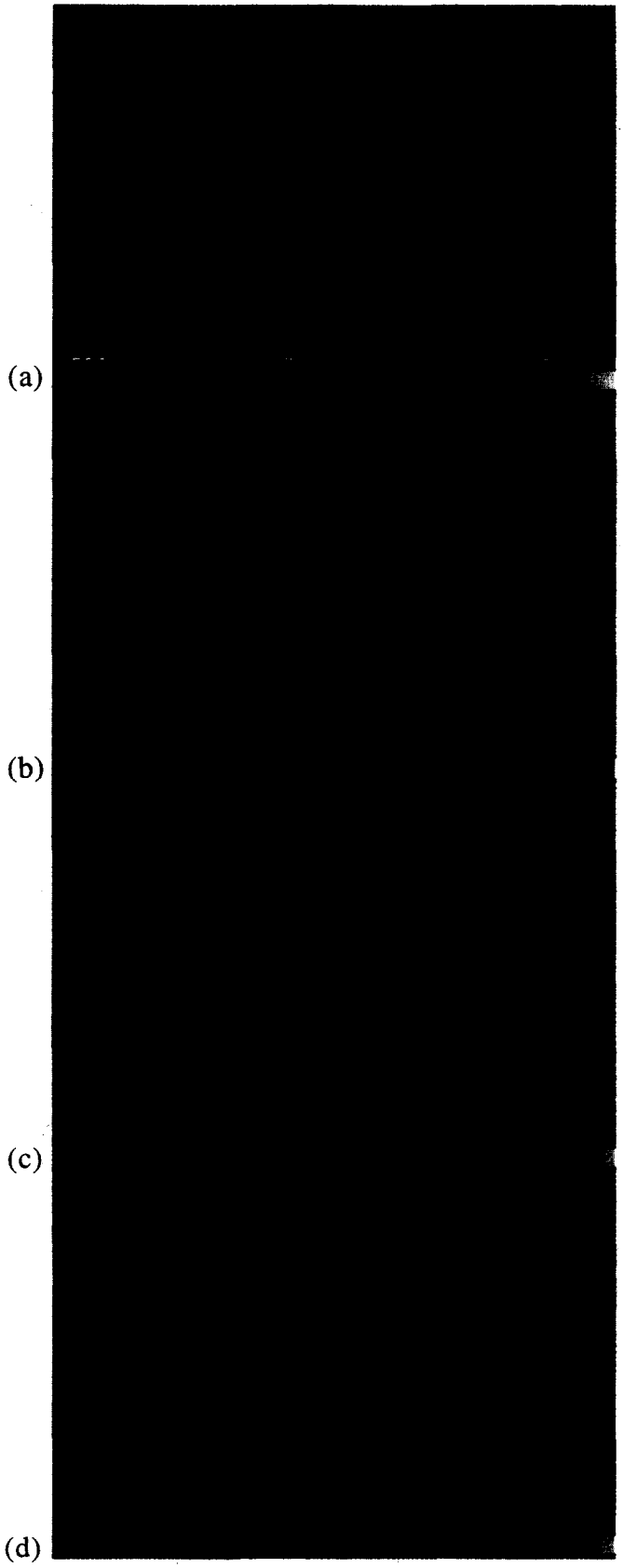

Fig. 6. The thermal field of the heated foil near the location of the string of particles at various values of one elevations. $Re_H = 9000$. The flow direction is from left to right. The color play interval is 10°C. (a) $y^+ = 21$; (b) $y^+ = 37$; (c) $y^+ = 45$; (d) flow without string.

Fig. 9. The thermal field of the heated foil near the location of two strings of particles. The color play interval is 10°C. $Re_H = 5400$, $D = 8d$. The flow direction is from bottom to top.

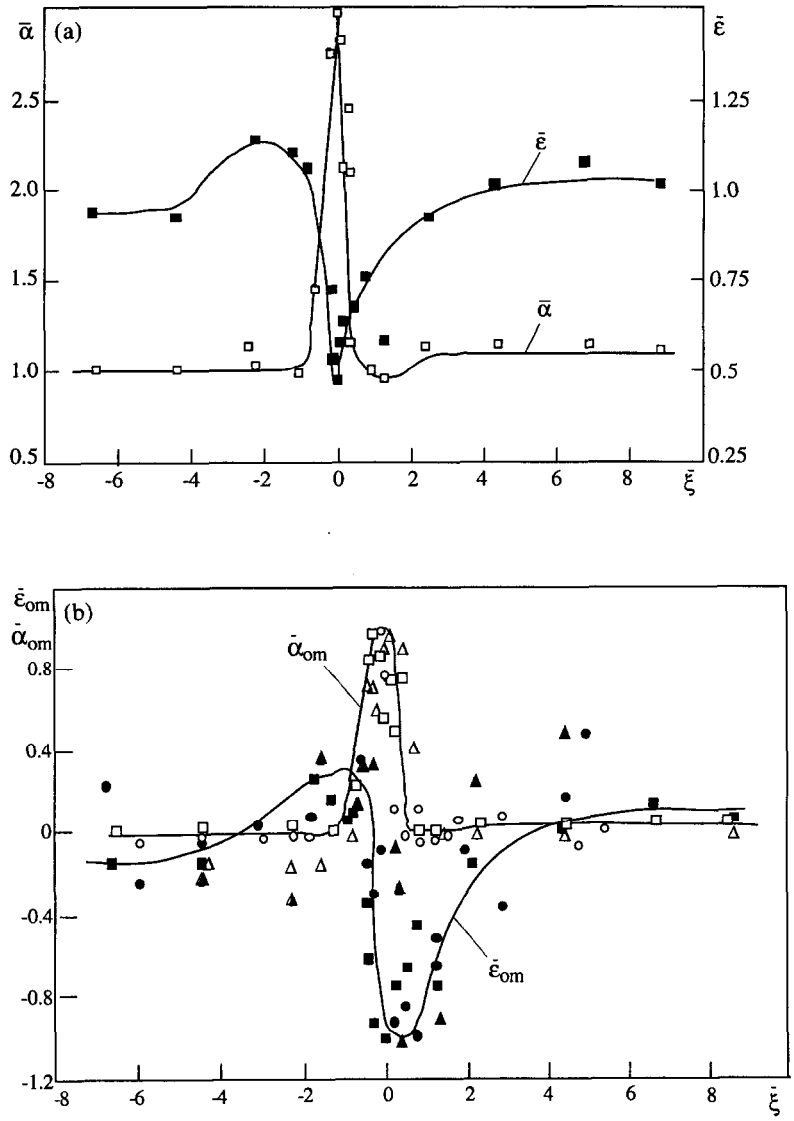

Fig. 4. Distributions of the heat transfer coefficient and temperature fluctuations at the wall near a single particle on the surface of the heated foil ($Re_H = 5150$). (a) $d = 4.75$ mm, □ $\bar{\alpha}$; ■ $\bar{\varepsilon}$; (b) $\bar{\alpha}_{0m}$: ○, □, △; $\bar{\varepsilon}_{0m}$: ●, ■, ▲, △, ▲—$d = 2.4$ mm; ○, ●—$d = 4.3$ mm; □, ■—$d = 4.75$ mm.

in a turbulent boundary layer is depicted in Fig. 11. The dependence of the heat transfer coefficient on the location $\bar{\xi}$ has two maxima located at the cross-section corresponding to the cylinder center and at some distance from it ($\bar{\xi} \approx 5$). The points corresponding to different distances of the cylinder from the wall, group near a single curve in the $\bar{\alpha}_{0m}$–$\bar{\xi}$ plane, except for the points corresponding to small values of h.

An increased elevation of the cylinder above the heater leads to a significant decrease in the maximum values of the heat transfer coefficient. The location of the second maximum $\bar{\alpha}_{0m} = f(\bar{\xi})$ is proportional to h^+.

5. MECHANISM OF HEAT REMOVAL FROM THE WALL NEAR A COARSE PARTICLE

Consider a possible mechanism of the effect of a single coarse particle on the rate of heat transfer in a turbulent boundary layer. For this purpose we study the developed turbulent flow without longitudinal pressure gradient along a flat plate.

Suppose that the particle (for example, a cylinder oriented along the z-axis) is located at a distance L from the leading edge of the heater at an elevation h over its surface (Fig. 12(a)). From a physical point of view, such a particle may affect the rate of heat transfer in two ways: by changing the velocity in the cross-section or as a result of a change in the velocity vector. The first effect is determined by the ratio of the particle characteristic scale d to the height of the fluid layer H. At a small value of d/H this effect is negligible. The change of flow geometry is accompanied by streamline bending. The latter leads to the emergence of a heterogenous field of centrifugal forces which affects the turbulent fluctuations.

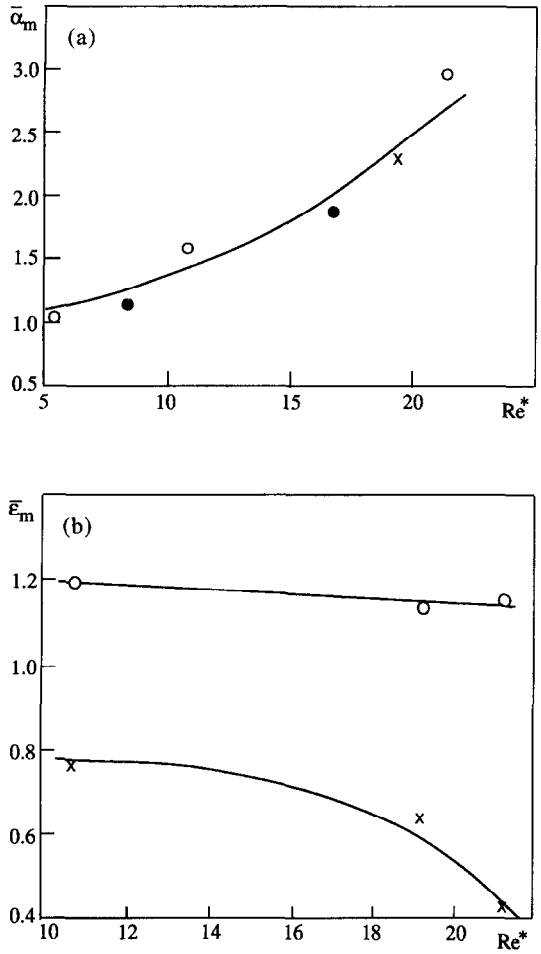

Fig. 5. Dependence of the heat transfer coefficient (the maximum value corresponding to the center of the particle) and maximum $\bar{\varepsilon}_{max}$ and minimum $\bar{\varepsilon}_{min}$ values of r.m.s. temperature fluctuations at the wall on Re^*. (a) The dependence of $\bar{\alpha}_m$ (Re^*) ●—Re_H = 5100 (steel), ×—Re_H = 5100 (glass), ○—Re_H = 8650 (steel). (b) The dependence of $\bar{\varepsilon}_m$ (Re^*). ○—$\bar{\varepsilon}_{max}$ and ×—$\bar{\varepsilon}_{min}$.

To estimate the effect of the change of the velocity vector on the heat transfer coefficient near a particle, consider the flow in the gap between the particle and the bottom plate (Fig. 12a). In domain I (abco′) the average velocity increases, from an initial value in the cross-section 'ab' to a maximum value in the cross-section 'co'', resulting in a negative longitudinal pressure gradient. Under these conditions the rate of heat transfer decreases [28]. The opposite effect is observed for the flow in domain II where the pressure gradient is positive at a constant Reynolds number.

Therefore, the heat transfer coefficient decreases in domain I and increases in domain II. However, as the measurements show (see Section 4), the real variation of the heat transfer coefficient is qualitatively different from the above explanation. The experiments show that the dominant factor in the heat transfer is the effect of centrifugal forces on the structure of the turbulent flow. As the analysis of the dynamic equations for the component of the tensor of turbulent stresses shows, the effect of the centrifugal force leads to an essential rearrangement of the field of turbulent fluctuations: all the components of fluctuation velocity, correlations $\overline{v_r' v_\varphi'}$, etc. are changed [35].

It is well known that in a stationary curved flow, the centrifugal forces acting on a fluid element are balanced by a centripetal pressure gradient, which causes modulation of turbulent fluctuations, which, in turn, affect the heat transfer. These effects manifest themselves clearly in flows in curved channels, where the heat transfer coefficient near the concave wall (the domain of turbulent fluctuations enhancement) is larger than that near the convex wall, where turbulent fluctuations are suppressed.

When $\partial^2\bar{p}/\partial r^2 > 0$, turbulent fluctuations are suppressed. Indeed, if the fluid element is pushed out of its equilibrium position by a random disturbance, it will be forced to return to its initial position by the pressure gradient, or centrifugal force. A different scenario appears if $\partial^2\bar{p}/\partial r^2 < 0$, when the centrifugal force promotes growth of the radial component of turbulent fluctuations. In this case motion of a fluid element from its position is accompanied by fluctuation growth, due to the excess centripetal pressure gradient or centrifugal force, respectively.

Taking into account the above mentioned considerations, let us estimate the pressure gradient distribution in the gap between a single particle and the bottom wall. Note that such an analysis does not require detailed knowledge of the fluid motion in the gap between the particle and the plate. It is necessary only to find regions where centrifugal force leads to an enhancement of turbulent fluctuations, or their suppression. For this purpose we use the Reynolds equations (for the radial velocity component) and the continuity equation. In cylindrical coordinates these equations are:

$$\bar{v}_r\frac{\partial\bar{v}_r}{\partial r}+\frac{\bar{v}_\varphi}{r}\frac{\partial\bar{v}_r}{\partial\varphi}+\frac{\bar{v}_\varphi^2}{r}=-\frac{1}{\rho}\frac{\partial\bar{p}}{\partial r}+\nu\left(\frac{\partial^2\bar{v}_r}{\partial r^2}+\frac{1}{r^2}\frac{\partial^2\bar{v}_r}{\partial\varphi^2}+\frac{1}{r}\frac{\partial v_r}{\partial r}-\frac{2}{r^2}\frac{\partial\bar{v}_\varphi}{\partial\varphi}-\frac{\bar{v}_r}{r^2}\right)-\frac{\partial\overline{v_r'^2}}{\partial r}-\frac{\partial\overline{v_r'v_\varphi'}}{\partial r}-\frac{\overline{v_r'^2}}{r}+\frac{\overline{v_\varphi'^2}}{r} \quad (9)$$

$$\frac{\partial\bar{v}_r}{\partial r}+\frac{1}{r}\frac{\partial\bar{v}_\varphi}{\partial\varphi}+\frac{\bar{v}_r}{r}=0 \quad (10)$$

where $\bar{v}_r$, $\bar{v}_\varphi$ and v_r', v_φ' are the radial and azimuthal components of the velocity vector (average and fluctuations, respectively), r is the radial and φ is the angular coordinate.

Consider the near-wall flow in the proximity of point B in front of the particle (Fig. 12(a)). The streamlines are inclined to the wall at less than the tangent to a circle at the same point. Therefore, the velocity vector is inclined to the wall at less than its

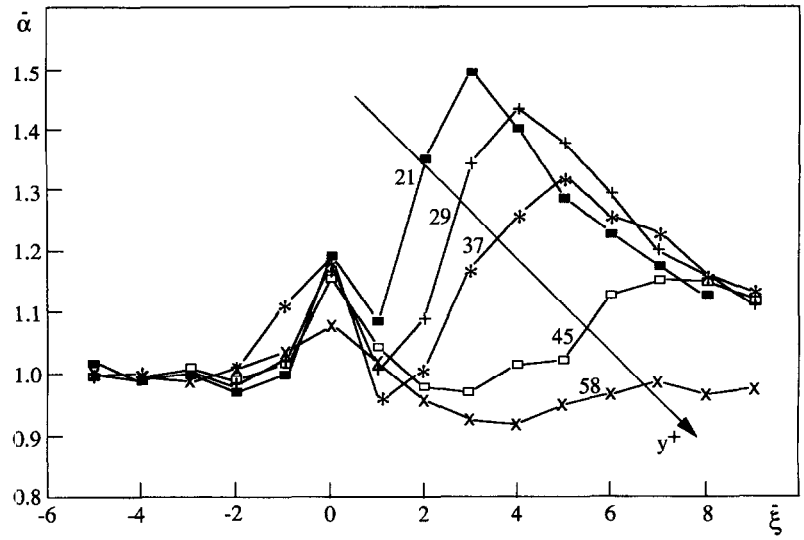

Fig. 7. Distributions of the heat transfer coefficient near the string of particles elevated above the wall ($d = 5$ mm, $Re_H = 9000$). ■—$h^+ = 21$, +—$h^+ = 29$, *—$h^+ = 37$, □—$h^+ = 45$, ×—$h^+ = 58$.

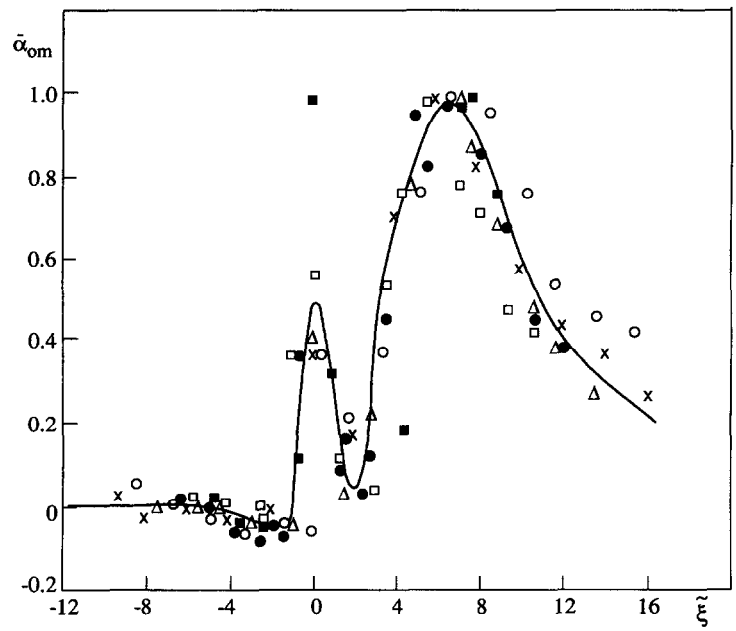

Fig. 8. The effect of a string of particles on the distribution of the heat transfer coefficient ($d = 5.0$ mm, $Re_H = 9000$). ×—$\bar{h} = 0.5$, ○—$\bar{h} = 0.59$, △—$\bar{h} = 0.68$, ●—$\bar{h} = 0.79$, □—$\bar{h} = 0.88$, ■—$\bar{h} = 1.07$.

tangential component. It is clear that the radial velocity component is directed towards the center of the particle and is negative: $\bar{v}_r < 0$. Since the radial velocity component equals zero at point B, the value of $\bar{v}_r$ increases, similar to $\bar{v}_r r = f(r)$. Indeed, since the product $\bar{v}_r r = 0$ at point B and at $\bar{v}_r r < 0$ at $r < r_B$ (r_B is the coordinate of point B), the value of $\bar{v}_r r = f(r)$ also increases as that of $\bar{v}_r$. Therefore, the derivative of the product $\bar{v}_r r$ is positive. As a result, we find, from the equation of continuity, that $\partial \bar{v}_\varphi / \partial \varphi < 0$. Within the limits $0 \leqslant r \leqslant h/\sin\varphi$ ($\varphi \leqslant \pi/2$) the radial velocity component varies in the range $0 \leqslant \bar{v}_r \leqslant \bar{v}_{rm}$, where $\bar{v}_{rm}$ is the value of $\bar{v}_r$ corresponding to $\varphi = 0$. Therefore, the derivative is $\partial \bar{v}_r / \partial \varphi < 0$. Note also that $\overline{v_r'^2} > 0$, $\overline{v_\varphi'^2} > 0$, and their values in the proximity of point B decrease, which results in the inequality $\partial \overline{v_r'^2} / \partial r < 0$.

We now estimate the contribution of the turbulent fluctuations to the radial pressure gradient. For this purpose, consider the terms of equation (9) which contain fluctuation velocities and their correlations. We begin with the equation of continuity of fluctuating velocities,

$$\frac{\partial v_r'}{\partial r} + \frac{1}{r}\frac{\partial v_\varphi'}{\partial \varphi} + \frac{v_r'}{r} = 0. \tag{11}$$

Multiplying equation (11) by v_r' and averaging, we have

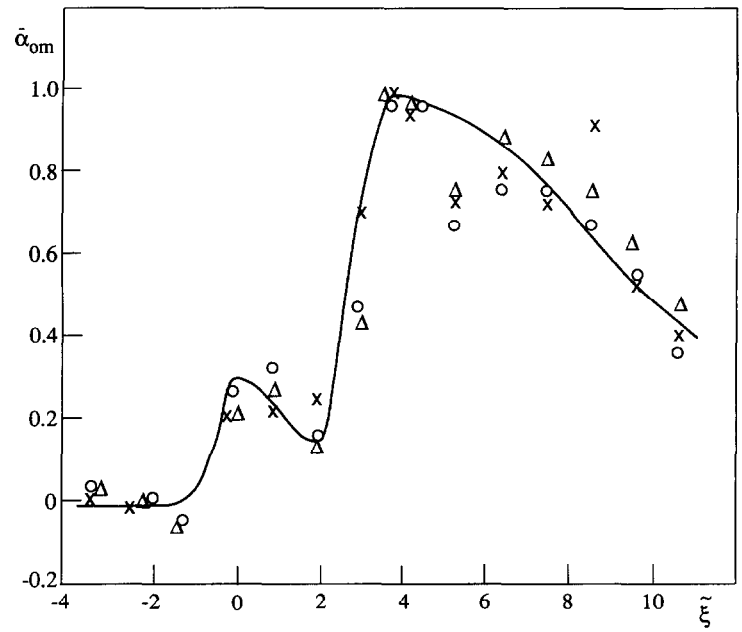

Fig. 10. The distribution of the heat transfer coefficient near two strings of particles located on the heater ($D = 4d$, $Re_H = 9000$). ×—$H = 0.037$ m, △—$H = 0.055$, ○—$H = 0.07$ m.

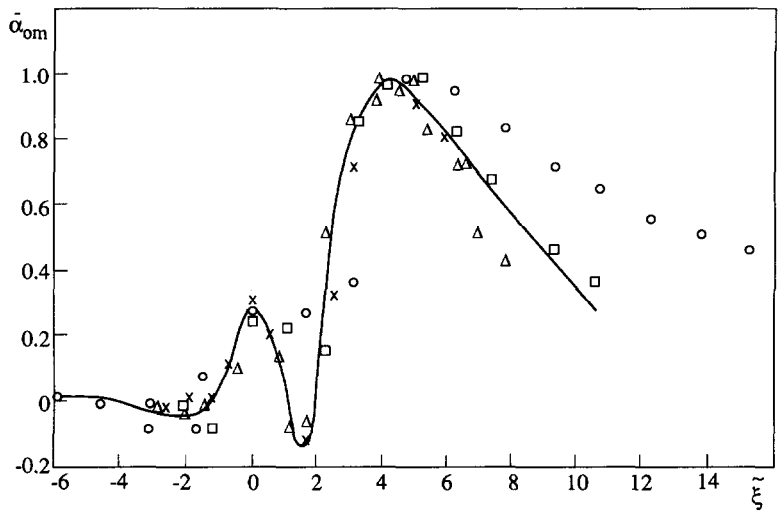

Fig. 11. The distribution of the heat transfer coefficient on the wall near a cylinder oriented in the spanwise direction in the turbulent boundary layer. ○—$h^+ = 28$, □—$h^+ = 41$, ×—$h^+ = 56$, △—$h^+ = 68$.

$$\frac{1}{2}\frac{\partial \overline{v_r'^2}}{\partial r} + \frac{1}{r}\overline{v_r' \frac{\partial v_\varphi'}{\partial \varphi}} + \frac{\overline{v_r'^2}}{r} = 0. \tag{12}$$

Since

$$\overline{v_r' \frac{\partial v_\varphi'}{\partial \varphi}} = \frac{\partial \overline{v_r' v_\varphi'}}{\partial \varphi} - \overline{v_\varphi' \frac{\partial v_r}{\partial \varphi}}$$

we can rewrite equation (12):

$$\frac{1}{2}\frac{\partial \overline{v_r'^2}}{\partial r} - \frac{1}{r}\overline{v_\varphi' \frac{\partial v_r'}{\partial \varphi}} + \frac{\overline{v_r'^2}}{r} = -\frac{1}{r}\frac{\partial \overline{v_r' v_\varphi'}}{\partial \varphi}. \tag{13}$$

Using equation (13) we rearrange the fluctuation terms in equation (9):

$$-\frac{\partial \overline{v_r'^2}}{\partial r} = \frac{1}{r}\frac{\partial \overline{v_r'^2 v_\varphi'}}{\partial \varphi} - \frac{\overline{v_r'^2}}{r} + \frac{\overline{v_\varphi'^2}}{r} = -\frac{1}{2}\frac{\partial \overline{v_r'^2}}{\partial r} + \frac{\overline{v_\varphi'^2}}{r} - \frac{1}{r}\overline{v_\varphi' \frac{\partial v_r'}{\partial \varphi}}. \tag{14}$$

Restricting ourselves only to the flow regimes where turbulence is the dominant factor and the effect of

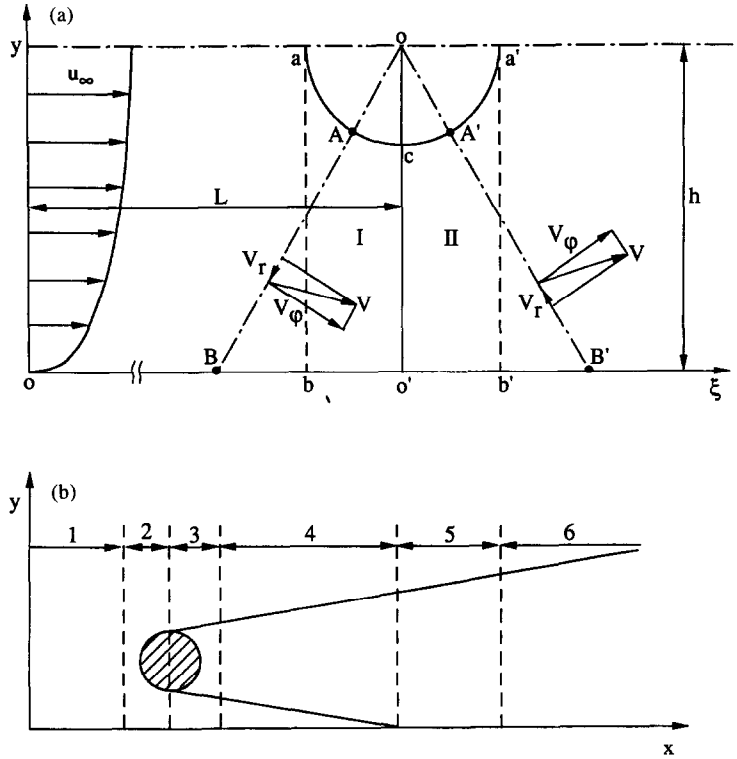

Fig. 12. Schematical description of the flow near a coarse particle. (a) The flow in the gap between the cylinder and the heater; (b) the flow behind a cylinder. 1 Unperturbed flow; 2 zone of fluctuations modulation; 3 zone of fluctuations stabilization; 4 intermediate zone; 5 zone of the interaction of the wake and the near-wall flow; 6 zone of damping of the turbulent fluctuations.

molecular viscosity is negligible, we obtain the following:

$$\frac{1}{\rho}\frac{\partial \bar{p}}{\partial r} = -\bar{v}_r\frac{\partial \bar{v}_r}{\partial r} - \frac{\bar{v}_\varphi}{r}\frac{\partial \bar{v}_r}{\partial \varphi} + \frac{\bar{v}_\varphi^2}{r} - \frac{1}{2}\frac{\partial \overline{v_r'^2}}{\partial r} + \frac{\overline{v_\varphi'^2}}{r} - \frac{1}{r}\overline{v_\varphi'\frac{\partial v_r'}{\partial \varphi}} \quad (15)$$

The first five terms on the r.h.s. of equation (15) are positive (see the estimations). To find the sign of the last term on the r.h.s. of equation (15), we assume that the turbulent fluctuations are isotropic, i.e. $v_\varphi' \approx v_r'$, and we get

$$\overline{v_\varphi'\frac{\partial v_r'}{\alpha\varphi}} \simeq \frac{1}{2}\frac{\partial \overline{v_r'^2}}{\partial \varphi}.$$

Accounting for the flow conditions in domain I (accelerating flow with a longitudinal pressure gradient), it is natural to assume that $\frac{1}{2}\partial \overline{v_\varphi'^2}/\partial\varphi \approx \overline{v_\varphi'\,\partial v_r'/\partial\varphi} < 0$. Accordingly, in region II (decelerating flow with a positive longitudinal pressure gradient) $\overline{v_\varphi'\,\partial v_r'/\partial\varphi} > 0$.

Thus the r.h.s. of equation (15) is positive. The absolute values of the terms on the r.h.s. of equation (15) decrease when the radial coordinate r increases.†

† Except for the derivative $\partial \overline{v_r'^2}/\partial r$, which may be assumed constant. The latter corresponds to a linear distribution of the turbulent fluctuations near the wall.

Accordingly, the value of $\partial \bar{p}/\partial r = f(r)$ decreases when r increases. For such a pressure gradient, the centrifugal forces enhance turbulent fluctuations. The latter leads to strong disturbances of the near-wall flow in the proximity of point B, disturbing of low-speed streaks, and formation of zones with small thermal resistance, which enhances the heat transfer rate.

Similarly, we can find the sign of the terms on the r.h.s. of equation (15) at point B′.

$$\bar{v}_r > 0;\quad \frac{\partial \bar{v}_r}{\partial r} < 0;\quad \bar{v}_\varphi > 0;\quad \frac{\partial \bar{v}_\varphi}{\partial \varphi} > 0;\quad \frac{\partial \overline{v_r'^2}}{\partial r} < 0;\quad \frac{\partial \bar{v}_r}{\partial \varphi} < 0;\quad \overline{v_\varphi'\frac{\partial v_r'}{\partial \varphi}} > 0. \quad (16)$$

Estimations, equation (16), show that at point B′ the terms on the r.h.s. of equation (15) have different signs. In this case, the gradient $\partial \bar{p}/\partial r = f(r)$ depends more weakly on r than that of point B. Therefore, the effect of centrifugal forces manifests itself more weakly near B′. In the case when $\partial^2 \bar{p}/\partial r^2 > 0$, centrifugal forces suppress the radial component of the fluctuations. This effect probably determines the change of heat transfer in domain II.

Similar effects manifest themselves near a spherical particle located on a flat surface. In this case, centrifugal forces affect the three-dimensional turbulent flow developing in the gap between the coarse spherical particle and the flat surface. Depending on the

distribution of the radial pressure gradient, this effect enhances or suppresses turbulent fluctuations and, accordingly, increases or decreases the heat transfer. Note that the effect of centrifugal forces on the heat transfer near a coarse particle manifests itself more clearly in a turbulent flow. At small Reynolds numbers this effect is smaller [24].

The above considerations are related to the flow in the close proximity of coarse particles. When a cylinder or a string of particles are placed on a flat surface, or above it, their effect on the heat transfer is also felt downstream. In this domain, the wake formed behind cylindrical particles interacts with the near-wall layer† (Fig. 12b). As can be seen in Fig. 12(b), six characteristic zones with different rates of heat transfer can be distinguished in the flow field.

For a coarse particle (in the region upstream of an unperturbed flow), the rate of heat transfer is determined by the local Reynolds number. In region 2, the centrifugal forces influence the fluctuations and cause sharp growth of the heat transfer coefficient. Zone 3 corresponds to the domain where the action of centrifugal forces stabilize the flow. Turbulence suppression in this region leads to a noticeable decrease in the heat transfer coefficient. In the intermediate zone 4 a turbulent wake behind the coarse particle does not interact with the wall. The interaction of this wake with the near-wall layer in zone 5 is accompanied by a sharp increase in the heat transfer coefficient and an appearance of the second maximum in $\bar{\alpha}_{0m} = f(\bar{\xi})$. In the sixth zone, the disturbances are damped and the flow is stabilized. The heat transfer coefficient in this zone is determined by the local value of the Reynolds number. The present model corresponds to the experimental data on the heat transfer coefficient distribution behind the string of coarse particles (Fig. 10) or cylinder (Fig. 11).

6. CONCLUSIONS

The effect of coarse particles on the heat transfer from a wall in a turbulent boundary layer was studied using infrared thermography. The heat transfer coefficient was investigated for different types of coarse particle arrangement (a single particle, a string of particles, etc.). Non-dimensional groups of parameters describing the heat transfer in a turbulent boundary layer with particles were determined. The experimental data on the heat transfer in a turbulent boundary layer were analyzed. A model of heat transfer in a turbulent boundary layer with coarse particles was proposed. The following results were obtained:

(1) A distribution of the heat transfer coefficient near a single coarse particle has two characteristic extrema: a minimum in front of the particle and a maximum near its center. The domain of minimum values of the heat transfer coefficient corresponds to the domain of maximum temperature fluctuations at the wall surface, whereas the maximum heat transfer coefficient corresponds to the domain of sharp decrease in temperature fluctuations on the wall.

(2) An increase in the gap between the particles and the bottom wall reduces the heat transfer coefficient.

(3) A distribution of the heat transfer coefficient, near a string of coarse particles or a cylinder oriented in the spanwise direction, has two characteristic maxima: near the centerline of the string and at some distance downstream. The absolute value of the heat transfer coefficient corresponding to the second maximum is larger than that for the first one.

(4) The effect of coarse particles on the heat transfer in a turbulent boundary layer is due to the centrifugal forces in the flow around curved particle surfaces. It is shown that such forces promote instability of the flow and cause bursting and an inrush of the cold fluid from the outer layer.

Acknowledgements—This research was supported by a grant from the Ministry of Science and the Arts, by the Technion VPR Fund, Israel, by the Mexico Energy Research Fund, and by the Fund for the Promotion of Research at the Technion. R. Rozenblit is partially supported by the Center for Absorption in Science, Ministry of Immigrants Absorption, State of Israel. L. P. Yarin is supported by the Israel Council for Higher Education.

REFERENCES

1. Kline, S. J., Reynolds, W. C., Schraub, F. A. and Rundstandler, P. W., The structure of turbulent boundary layer. *Journal of Fluid Mechanics*, 1967, **70**, 741–773.
2. Head, M. R. and Bandyopadhyay, P., New aspects of turbulent-boundary structure. *Journal of Fluid Mechanics*, 1981, **107**, 297–338.
3. Gad-el-Hak, M. and Bandyopadhyay, P. R., Reynolds number effect in wall-bounded turbulent flows. *Applied Mechanics Review*, 1994, **47**, 307–365.
4. Falco, R. E., A coherent structure model of the turbulent boundary layer and its ability to predict Reynolds number dependence. In *Turbulent Flow Structure Near Walls*. Cambridge University Press, Cambridge, 1991.
5. Kaftori, D., Hetsroni, G. and Banerjee, S., Funnel shaped vortical structure in wall turbulence. *Physics of Fluids*, 1994, **6**, 3035–3050.
6. Yarin, L. P. and Hetsroni, G., On bursting of coherent structure in fluid flow. *Transactions of the ASME, Journal of Fluids Engineering* (submitted).
7. Kline, S. J., The role of visualization in the study of the structure of the turbulent boundary layer. In *Coherent Structure of Turbulent Boundary Layers*, ed. C. R. Smith and D. E. Abbott. Lehigh AFOSR, 1978, pp. 1–26.
8. Cantwell, B. J., Organized motion in turbulent flow. *Annual Review of Fluid Mechanics*, 1981, **13**, 457–515.
9. Nezu, I. and Nakagawa, H., *Turbulence in Open-Channel Flows*. Balkema, Rotterdam, 1993.
10. Hetsroni, G., Yarin, L. P. and Kaftori, D., A mechanistic model for heat transfer from a wall to a fluid. *International Journal of Heat and Mass Transfer*, 1996, **39**, 1475–1478.
11. Gore, R. A. and Crowe, C. T., Effect of particle size on modulating turbulent intensity. *International Journal of Multiphase Flow*, 1989, **2**, 279–285.
12. Hetsroni, G., Particle-turbulence interaction. *International Journal of Multiphase Flow*, 1989, **5**, 735–746.

† The flow behind a system of spheres located on a flat surface has a number of peculiarities due to formation of secondary flows [29].

13. Tsuji, Y. and Morikawa, Y., LDV-measurements of an air-solid two-phase flow in horizontal pipe. *Journal of Fluid Mechanics*, 1982, **120,** 358–409.
14. Lee, S. L. and Durst, F., On the motion of particles in turbulent duct flow. *International Journal of Multiphase Flow*, 1982, **8,** 125–146.
15. Tsuji, Y., Morikawa, Y., Tanaka, T., Kaximine, K. and Nishida, S., Measurements of unaxisymmetric jet laden with coarse particles. *International Journal of Multiphase Flow*, 1988, **14,** 565–574.
16. Shuen, J. S., Solomon, A. S., Zhang, Q. F. and Faeth, G. M., Structure of particle-laden jet : measurements and predictions. *AIAA Journal*, 1985, **23,** 396–404.
17. Sun, T. V. and Faeth, G. M., Structure of turbulent bubbly jets. Methods and centerline properties. *International Journal of Multiphase Flow*, 1986, **12,** 99–114.
18. Parthasarathy, R. N. and Faeth, G. M., Structure of turbulent particle-laden water jet in still water. *Journal of Fluid Mechanics*, 1987, **220,** 485–537.
19. Yarin, L. P. and Hetsroni, G., Turbulence intensity in dilute two-phase flows—3. The particles-turbulence interaction in dilute two-phase flow. *International Journal of Multiphase Flow*, 1994, **1,** 27–44.
20. Rashidi, M., Hetsroni, G. and Banerjee, S., Particle-turbulence interaction in a boundary layer. *International Journal of Multiphase Flow*, 1990, **16,** 935–949.
21. Kaftori, D., Structures in the turbulent boundary layer and their interaction with particles. Ph.D. thesis, University of California, Santa-Barbara, CA, 1993.
22. Grass, A. J., Stuart, R. G. and Mansor, D. B., Vortical Structures and coherent motion in turbulent flow over smooth and rough boundaries. *Philosophical Transactions of the Royal Society of London A*, 1992, **336,** 35–69.
23. Hetsroni, G. and Rozenblit, R., Heat transfer to a liquid-solid mixture in a flume. *International Journal of Multiphase Flow*, 1994, **4,** 671–689.
24. Hetsroni, G., Rozenblit, R. and Lu, D. M., Heat transfer enhancement by a particle on the bottom of a flume. *International Journal of Multiphase Flow*, 1995, **21,** 963–984.
25. Owen, P. R. and Thomson, W. R., Heat Transfer across rough surface. *Journal of Fluid Mechanics*, 1963, **15,** 321–334.
26. Yaglom, A. M. and Kader, B. A., Heat and mass transfer between a rough wall and turbulent fluid flow at high Reynolds and Peclet number. *Journal of Fluid Mechanics*, 1974, **62,** 601–623.
27. Hirota, M., Fujita, H. and Yokosawa, H., Experimental study on convective heat transfer for turbulent flow in a square duct with a ribbed rough wall. *Journal of Heat Transfer, Transactions of the ASME*, 1994, **116,** 332–340.
28. Zukauskas, A., *High-Performance Single-Phase Heat Exchanges*. Hemisphere, New York, 1989.
29. Schlichting, H., *Boundary Layer Theory*, 1979, 7th edn. McGraw-Hill, New York.
30. Zukauskas, A., Enhancement of forced convection heat transfer in viscous fluid flows. *International Journal of Heat and Mass Transfer*, 1994, **37,** 207–212.
31. Aliaga, D. A., Lamb, J. P. and Klein, D. E., Convection heat transfer distributions over plates with square ribs from infrared thermography. *International Journal of Heat and Mass Transfer*, 1994, **3,** 365–374.
32. Lion, T. M. and Wang, W.-B., Laser holographic interferometry study of developing heat transfer in a duct with a detached rib array. *International Journal of Heat and Mass Transfer*, 1995, **1,** 91–100.
33. Webb, R. L., *Principles of Enhanced Heat Transfer*. Wiley, New York, 1994.
34. Zhang, X., Stasiek, J. and Collins, M. W., Experimental and numerical analysis of convective heat transfer in turbulent channel flow with square and circular columns. *Experimental Thermal and Fluid Science*, 1995, **10,** 229–237.
35. Ustimenko, B. P., *The Process of Turbulent Transfer in Vortex Flows*. Nauka, Alma-Ata, 1977, pp. 141–146.